Cleaning and Heat-Treatment Effects on Unalloyed Titanium Implant Surfaces

Deepak V. Kilpadi, PhD[1]/Jack E. Lemons, PhD[2]/Jun Liu, PhD[3]/Ganesh N. Raikar, PhD[4]/
Jeffrey J. Weimer, PhD[5]/Yogesh Vohra, PhD[6]

This study tested the following hypotheses: (1) acid-cleaned and passivated unalloyed titanium implants have higher surface energies (which are considered desirable for bone implants) than ethanol-cleaned titanium; (2) higher temperatures of heat treatment of unalloyed titanium result in higher surface energies; and (3) these changes can be related to changes in surface composition and roughness. Thus, unalloyed titanium specimens were either acid-cleaned and passivated (CP) or ethanol-cleaned (Et). Each set was then divided into 3 groups and heat-treated for 1 hour at 316°C (600°F), 427°C (800°F), and 538°C (1,000°F), respectively. Surface roughness values for each of these groups were determined using atomic force microscopy, while surface compositions were determined using Auger electron, x-ray photoelectron, and Raman spectroscopic techniques. Surface energies were estimated using a 2-liquid geometric mean technique and correlated with surface roughness, elemental composition, and elemental thickness. The CP surfaces were slightly rougher than the Et specimens, which had greater oxide thickness and hydrocarbon presence. The surface oxides were composed of TiO_2, Ti_2O_3, and possibly titanium peroxide; those heat-treated at 427°C or above were crystalline. The CP specimens had carbonaceous coverage that was of a different composition from that on Et specimens. The CP specimens had significantly higher surface energies, which showed statistically significant correlations with oxide thickness and carbonaceous presence. In conclusion, ethanol cleaning of unalloyed titanium dental implants may not provide optimal surface properties when compared to cleaning with phosphoric acid followed by nitric acid passivation. (Int J Oral Maxillofac Implants 2000;15:219–230)

Key words: *ethanol, passivation, surface characterization, temperature, titanium*

[1]Adjunct Research Assistant Professor, Joint Materials Science PhD Program of The University of Alabama System; and Department of Biomaterials, University of Alabama at Birmingham.
[2]Professor, Joint Materials Science PhD Program of The University of Alabama System; and Department of Biomaterials, University of Alabama at Birmingham.
[3]Researcher, Department of Physics, University of Alabama at Birmingham.
[4]Manager, Surface Analysis and Optical Spectroscopy Laboratory, University of Utah, Salt Lake City, Utah.
[5]Associate Professor, Joint Materials Science PhD Program of The University of Alabama System; and Department of Chemistry and Departments of Chemical and Materials Engineering, University of Alabama at Huntsville.
[6]Professor, Joint Materials Science PhD Program of The University of Alabama System; and Department of Physics, University of Alabama at Birmingham.

Reprint requests: Dr D.V. Kilpadi, Department of Biomedical Engineering, University of Alabama at Birmingham, 370 Hoehn, 1075 13th Street South, Birmingham, AL 35294. Fax: (205) 975-4919. E-mail: dkilpadi@uab.edu

The use of metallic implants for dental applications has been increasing, partly because of the possibility of close bone apposition.[1] Increased bone contiguity has been shown to provide characteristics for enhancing long-term implant viability. From a biomaterials perspective, surface roughness, composition, and energy can influence biologic responses and, hence, clinical function.[2,3] For example, osteoblasts have been shown to proliferate on rougher surfaces.[3] Also, surface composition and roughness can affect surface energy. Surfaces with higher surface energies exhibit enhanced wetting behavior, which is thought to result in better interactions with the moieties that are important for osteal responses.

National and international standards on the properties of metallic biomaterials for surgical implants are fairly broad, allowing for several possible procedures prior to implantation—cleaning, passivation, and sterilization—that may include exposure to

Table 1 Surface Roughness Parameters Examined with Atomic Force Microscopy

Parameter	Description
Z-range	Distance between the highest and lowest points within a given area
R_q	Standard deviation of height measurements relative to the mean height within a given area
R_a	Mean value of the surface relative to the center plane (the center plane is flat and divides the enclosed volume of the image surface into 2 equal parts)
R_{max}	Difference in height between the highest and lowest points relative to the mean plane (the mean plane is determined from a first-order least-squares-fit of height data, thereby minimizing variance of image data about this plane)
Surface area difference	Percentage increase of 3-dimensional area relative to 2-dimensional image area (14 μm × 14 μm)

elevated temperatures.[1,4] Previous studies show that the combination of passivation and dry-heat sterilization at 205°C, after cleaning in phosphoric acid, increases surface energy of titanium, while the absence of passivation affects subsequent oxide growth.[5,6] Also, coating techniques such as ion beam sputtering or plasma spraying include heat treatments in the range of about 500°C to 600°C of the coated implant to optimize coating properties.[7] These presurgical procedures can alter the surface characteristics considered critical to biocompatibility. The current study investigated the influence of higher temperatures of heat treatments on the surface energy, roughness, and composition of unalloyed titanium specimens that were either previously acid-cleaned and passivated or ethanol-cleaned.

MATERIALS AND METHODS

Unalloyed grade 2 titanium was wet-ground using 320- through 600-grit silicon carbide papers. Specimens were then either ethanol-cleaned (Et)—ultrasonically cleaned in 95% ethanol for 10 minutes and allowed to air-dry—or acid-cleaned and passivated (CP)—cleaned in 50% (volume) phosphoric acid for 30 minutes, ultrasonically cleaned in deionized water for 10 minutes, passivated in 30% (volume) nitric acid at room temperature for 20 minutes, ultrasonically cleaned again in deionized water for 10 minutes, and finally air-dried. Each sample was divided into 3 groups and heated independently in air for 1 hour at temperatures of 316°C (600°F), 427°C (800°F), and 538°C (1,000°F), respectively, and then allowed to cool to room temperature. All specimens were then stored in a dessicator until analyzed.

Atomic Force Microscopy

Surfaces were examined for microtopographic characteristics with atomic force microscopy (AFM) (Nanoscope III, Digital Instruments, Santa Barbara, CA) using SiN cantilever probes with a constant force of 0.58 N/m and a scan rate of 4 Hz. The tips had a nominal radius of 20 to 40 nm. Roughness was quantified through multiple analyses of 14 × 14 μm^2 area scans (Table 1). Five regions per sample type were examined within a 4-hour period at similar room temperature and humidity. No image processing was done.

Solid Surface Tension

Values for solid surface tension (γ_s) were determined using contact angles of drops of ultrapure diiodomethane and distilled water on specimen surfaces that were measured using a goniometer setup (NRL-100, Ramé-Hart, Mountain Lakes, NJ). At least 8 measurements per liquid and surface type were made to provide data for statistical analysis. Surface energy was determined 1 to 4 days after specimen preparation. Previous studies on the influence of storage time showed that time-dependent variance of γ_s, if any, occurred within the first 24 hours of storage; the γ_ss of dry heat–sterilized specimens did not change substantially with dry storage.[8] To minimize effects of alterations caused by the environment at room temperature and humidity, all surfaces were examined within a few hours of each other at room temperature (23°C to 24°C).

The total surface tensions (γ_t) of the test liquids (distilled water = 72.8 dyne cm^{-1} and diiodomethane = 50.8 dyn cm^{-1}) were measured using the De Nöuy technique (DCA-312, Cahn Instruments Inc, Cerritos, CA) and were found to be similar to values cited in the literature.[9] The polar (γ_p) and dispersive (γ_d) components (water γ_p = 50.3 dyne cm^{-1}; water γ_d = 22.5 dyn cm^{-1}; diiodomethane γ_p = 2.3 dyne cm^{-1}; diiodomethane γ_d = 48.5 dyne cm^{-1}) were taken to be the same as values in the literature.[9] The 2-liquid geometric mean equation, recommended for examining high-surface energy surfaces, was used to determine γ_d, γ_p, and γ_t of the titanium surfaces.[10] Acid-cleaned polytetrafluoroethylene (PTFE) was examined for calibration and as a check of methodology.[9]

Auger Electron Spectroscopy

Auger electron spectroscopic (AES) analyses were done to determine surface elemental composition of the samples. This was done using a JAMP-30 Auger system (JEOL, Tokyo, Japan) at a base pressure of 2×10^{-7} to 3×10^{-7} Pa. The electron beam current was maintained at about 3.5×10^{-7} A, with an accelerating voltage of 10 kV. All results were obtained at a beam take-off angle of 30 degrees. A modulation potential of 5 V peak-to-peak was used to obtain the data in the differentiated form.

Survey scans (0 to 2,000 eV) were taken both prior to and after depth profiling. Surface layers were sputtered away in 1-second cycles, using a 3 kV, 30 mA argon ion beam at a pressure of 7 mPa. The difference between maximum and minimum intensity of chosen peaks was plotted for after each sputtering cycle. The sputter rate was calibrated using a 1,000 Å Ta_2O_5 oxide layer on a Ta substrate. Oxide depth was estimated by measuring the number of cycles for the oxygen peak to reach half the maximum concentration.[11] Depths for other elements were determined by the number of cycles taken for the concentration to drop to half the difference between maximum and minimum values. Five spots per surface type were examined.

X-ray Photoelectron Spectroscopy

X-ray photoelectron spectroscopy (XPS) was used to elicit surface elemental and chemical information. The XPS analyses (Perkin-Elmer ESCA 5400, Norwalk, CT) were conducted at a take-off angle of 45 degrees with a base main chamber pressure of less than 7×10^{-8} Pa. The source was MgK-α radiation at 15 kV and 300 W. Survey scans were done at a pass energy of 89.54 eV and a range of 0 to 1,100 eV. Atomic concentrations were determined from subsequent multiplex spectral scans at a pass energy of 17.9 eV. Two regions per surface type were examined, and quantitative data were obtained from one of these regions. High-resolution scans at a pass energy of 8.95 eV were used to examine elements with an atomic percentage greater than 3%; peak fitting for the C 1s, O 1s, and Ti 2p peaks was done to determine peak separations and full-width half-maximum (FWHM) values, using software on the XPS system.

Raman Spectroscopy

Raman spectroscopy was used to obtain surface chemical and structural information. Replicate specimens were examined using a micro-Raman spectroscopy system (Dilor, Lille, France). A tunable argon laser (Coherent Innova 70, Santa Clara, CA) with a wavelength of 514.6 nm was used. Two spots per surface type were examined at a laser power of 20 mW with a collection time of 200 seconds.

Statistical Procedures

Two-way analysis of variance was used to determine whether effects of surface treatment, temperature of heat treatment, and interaction between surface treatment and temperature were present (interaction alludes to the dependence of the effect of one factor on the other). If differences were present, means were ranked using the Newman-Keuls technique. When comparing surface energy data, 2-way analysis of variance (ANOVA) was done using no replication (ie, only the means for each of the 6 samples were used), unlike other 2-way ANOVA comparisons, where all of the data were used. Differences and ranking among the surface energy data were determined using the Bonferroni *t* test.

Correlation coefficients were used to relate surface roughness, composition, and elemental depths to surface energy. The coefficients were initially tested for significance (ie, whether they were different from 0) and then compared using the Fisher *z*-test.

RESULTS AND DISCUSSION

Atomic Force Microscopy

Roughness values for the surfaces are given in Table 2. The temperature of heat treatment did not alter surface roughness in either CP or Et specimens. However, CP specimens had higher R_q values when compared to the Et samples ($P = .03$). These findings support previous findings where acid-cleaned, passivated, and dry heat–sterilized specimens were rougher than those that were not passivated.[6] With more specimens, it is possible that Z-range ($P = .08$) and R_a values ($P = .06$) also may have been significantly higher for CP specimens. No differences were noted for R_{max} and surface area difference parameters.

Dissimilar surface profiles can have the same roughness parameter value.[12] Thus, a number of roughness parameters were examined in this study. The Z-range parameter, and to a slightly lesser extent, R_{max}, are sensitive to high peaks and deep valleys. The R_a and R_q parameters measure average deviation from a reference plane. The R_q parameter is more sensitive than R_a to occasional peaks or valleys and tends to be greater than the corresponding R_a values for a given surface. This was consistent in the present study: Z-range > R_q > R_a for all surfaces.

Increased surface roughness has been associated with greater osteoblastic activity.[2] Although the critical level of difference of roughness magnitudes

Table 2 Surface Roughness

	Temperature of heat treatment						2-way ANOVA *P* values		
	316°C		428°C		538°C			Temperature	
Parameter	CP	Et	CP	Et	CP	Et	CP vs Et	effect	Interaction
Z-range (nm)	880 ± 10	770 ± 10	850 ± 10	660 ± 10	850 ± 10	770 ± 10	.08	.68	.79
R_q (nm)	180 ± 30	130 ± 20	160 ± 30	110 ± 10	160 ± 30	130 ± 10	.03	.59	.94
R_a (nm)	140 ± 20	110 ± 20	120 ± 20	90 ± 10	130 ± 30	110 ± 10	.06	.49	.95
R_{max} (nm)	870 ± 70	760 ± 100	790 ± 50	640 ± 60	830 ± 130	760 ± 70	.12	.47	.88
Surface area difference (%)	4.1 ± 0.5	5.1 ± 0.9	4.3 ± 0.3	2.7 ± 0.2	4.5 ± 1.0	4.9 ± 0.7	.92	.15	.17

CP = cleaned in phosphoric acid and passivated in nitric acid; Et = cleaned in ethanol.

Table 3 Surface Energy Estimation

		Solid surface tension, dyn/cm		
Samples	Temperature (°C)	γ_p	γ_d	γ_t
CP samples	316	22.9 ± 0.2	23.6 ± 0.2	46.5 ± 0.3
	427	26.8 ± 0.2	28.8 ± 0.6	55.6 ± 0.6
	538	26.6 ± 0.1	24.3 ± 0.1	50.9 ± 0.1
Et samples	316	12.3 ± 0.2	28.2 ± 0.3	40.5 ± 0.4
	427	18.9 ± 0.1	24.7 ± 0.1	43.6 ± 0.2
	538	21.1 ± 0.2	23.3 ± 0.2	44.4 ± 0.2
P, CP versus Et		.03	.95	< .05
P, temperature effects		.13	.68	.20

CP = cleaned in phosphoric acid and passivated in nitric acid; Et = cleaned in ethanol; γ_p = polar solid surface tension; γ_d = dispersive solid surface tension; γ_t = total solid surface tension.

that influence biologic response has not as yet been established, cells tend to respond most actively to structures that approach their size.[13] The scan lengths used in this study, along with the resolution afforded by AFM, allowed for the study of surface roughness because of structures that were of the same order of magnitude as cells.

Solid Surface Tension

Table 3 shows the γ_s for the sample surfaces. Although estimation of surface energy can be affected by surface roughness,[14,15] no statistically significant correlations between surface roughness parameters and surface energy were detected in this study. Therefore, surface energies were not corrected for surface roughness.

Dispersive solid surface tension was not affected by temperature or surface treatment. Grain structure and mechanical strain, which can be altered with exposure to elevated temperature, are thought not to affect the dispersive component of surface energy.[16] The CP specimens had consistently higher γ_p, and hence γ_t (the sum of γ_p and γ_d), values than the corresponding Et specimens. In fact, even the CP specimens with the lowest γ_p had a value greater than the Et sample with the largest polar component. Although effects of exposures at various temperatures were not statistically significant, possibly because of similar γ_p values for CP specimens heat-treated at 538°C (538CP) and 427°C (427CP), higher temperatures resulted in higher mean γ_p for both groups of surface treatment (although there appeared to be an upper limit, as shown by the comparable 427CP and 538CP values). Similarly, CP surfaces had higher total solid surface tension values (γ_t) than Et samples. These findings corroborated results from a previous study on cleaned, passivated, and dry heat–sterilized specimens where γ_p was correlated with total solid surface tension.[6]

The surface energy parameter has been shown to be a useful indicator for predicting biologic response.[2,3] However, surface energies are not unique; that is, different surface compositions may result in a similar surface energy value. In addition to modulating biologic response indirectly by altering surface wettability, surface composition can affect biologic response directly through specific interactions with the biologic milieu.

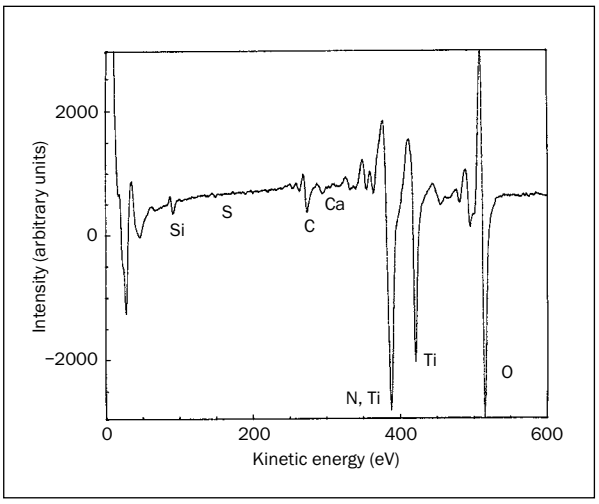

Fig 1 Representative pre-sputter Auger spectrum (538CP).

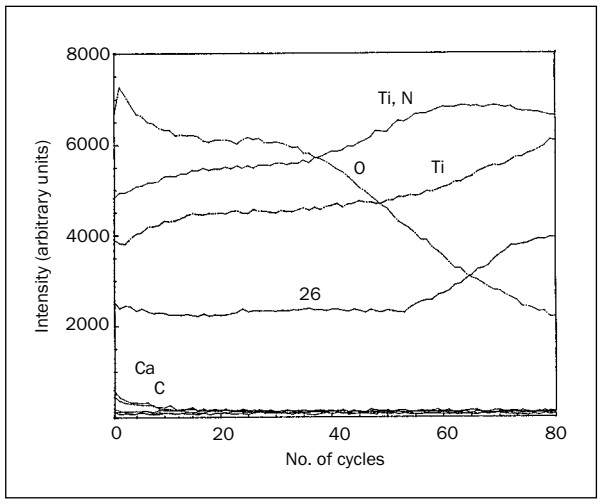

Fig 2 Representative depth profile of 538CP specimens. The profile marked 26 corresponds to a minor titanium peak at about 26 eV.

Auger Electron Spectroscopy

Surface composition analysis using Auger spectroscopy showed the presence of oxygen, titanium, and carbon (Fig 1). There were also trace levels of silicon, sulfur, calcium, and phosphorus on some of the specimens. Removal of adsorbed oxygen, water, and oxygen-containing carbonaceous species in the initial stages of vacuum exposure and sputtering caused the oxygen profile to decrease, as seen in Fig 2. It reached a plateau, indicating the presence of a subsurface zone of stoichiometric oxide. Further sputtering lead to a gradual drop in the oxygen intensity in the profile. This probably indicates that the oxide boundary is not abrupt, unlike the Ta_2O_5-Ta boundary (recall Ta_2O_5 was used to estimate the sputtering rate). Differences in the sputtering rates of the oxides and metallic titanium, along with crater effects, may have contributed to the broadening of the depth profile. Other possible contributions may have been the result of differences in the readsorption of sputtered moieties, ionic implantation and atomic mixing, and shadowing related to asperities/surface roughness.[17]

Depth profiling results are provided in Table 4. Oxide thickness increased, as expected, with temperature of exposure for both CP and Et specimens. Two-way ANOVA confirmed that no interaction effects were present and that the oxide thicknesses measured using the half-maximum method were affected by temperature as well as surface treatment. The Et samples had thicker oxide layers than the CP ones. This agrees with previous studies in which unpassivated but dry heat–sterilized (at 205°C) samples had smoother and thicker oxide layers than those that had also undergone the passivation process.[5,6]

Specimens that were heat-treated (both CP and Et) at 316°C did not show a visual color change; that is, the surface before and after heat treatment retained the original metallic gray color. The specimens heated to 427°C had a uniform golden color, and surfaces that were heat-treated at 538°C were blue, with areas of varying shades of purple and some white. These colors are a result of the interference of incident white light and can be related to the relative thickness of crystalline surface oxide layers.[18] A previous study by Fukuzuka et al using ellipsometry data indicated that the surface oxide layer on titanium was colorless when its thickness was below 100 Å, yellow between 100 and 250 Å, blue between 250 and 700 Å, blue-green between 700 and 1,700 Å, and white when the oxide was thicker than 1,700 Å.[18] The variation in color, from blue to white, of specimens heated at 538°C was probably the result of differing local oxide thickness that was attributed to varying heating/cooling rates, which are thought to be dependent on local thermal gradients. Also, a previous corrosion study had shown that titanium specimens that were heat-treated at 538°C were more likely to corrode than those exposed to lower temperatures.[19] It is possible that microcracks at the oxide-metal interface, caused by stresses from differential thermal expansion, may have facilitated the increase in the equilibrium corrosion potential (E_{corr}). These microcracks may also have facilitated differential oxide growth, resulting in a surface oxide layer of varying thickness and, hence, varying shades

Table 4 Auger Depth Profile Results

	Temperature of heat treatment						2-way ANOVA *P* values		
	316°C		427°C		538°C		Temperature		
Element	CP	Et	CP	Et	CP	Et	effects	CP vs Et	Interaction
Oxygen	69.4 ± 7.8	109.8 ± 22.1	93.2 ± 11.6	172.6 ± 7.3	116.8 ± 17.2	231.4 ± 56.6	< .01	< .01	> .1
Oxygen plateau	17.0 ± 17.0	69.7 ± 25.5	42.5 ± 6.8	98.6 ± 11.9	66.3 ± 15.3	68.0 ± 34	.34	.02	.42
Carbon	7.7 ± 2.2	16.8 ± 8.7	4.6 ± 0.5	9.2 ± 1.9	5.8 ± 1.9	9.0 ± 1.2	.33	.03	.93

Values are shown as mean ± standard error in Å.

Table 5 Auger Elemental Thickness Profile and Surface Energy

		Correlation coefficient (r)	
Series	Surface tension type	Oxide thickness	Carbon
CP only	γ_d	—	—
	γ_p	p	—
	γ_t	—	n
Et only	γ_d	n	—
	γ_p	p	—
	γ_t	p	—
All	γ_d	—	—
	γ_p	—	n
	γ_t	—	n

CP = cleaned in phosphoric acid and passivated in nitric acid; Et = cleaned in ethanol; γ_d = dispersive solid surface tension; γ_p = polar solid surface tension; γ_t = total solid surface tension; p = positive correlation; n = negative correlation.

of color. As it was not possible to isolate regions of different colors using the black-and-white video output that is inherent with electron microscopic imaging, multiple random sites were examined on a given surface. It was not possible to discern nano- or microcracks, if any, that may have propagated and manifested at the specimen surfaces with either AFM or SEM because of the relative roughness of all the surfaces and the relatively long AFM scan lengths used in this study.

Similarities in color (indicative of similar oxide thicknesses) of CP and Et specimens treated at similar temperatures could have been attributed to the thickness range (about 150 to about 450 Å) that can result in a similar reflected light interference (Table 4).[18] Also, relative differences in surface roughness and composition may have altered relative sputtering rates and contributed to differences in estimated oxide thickness.

There was a slight variance from the results presented by Fukuzuka in that these particular colors and the measured oxide thicknesses did not fully agree with the Fukuzuka model. This difference may be the result of the Auger depth profile being calibrated using standard tantalum oxide specimens, which may not have fully represented the actual sputtering rate of the titanium surfaces. However, while quantitative comparisons were not possible with other studies per se, the trends were comparable. The Newman-Keuls test for multiple comparisons showed that 538Et and 427Et had the thickest oxide layers. Despite obvious thickness differences between the oxide layers of these surfaces, as substantiated by color differences, the large standard error for 538Et prevented determination of any statistical difference. The magnitude of this variation was in agreement with the different color shadings on the surface. No other statistically significant differences in depth profiles were noted, although color differences were clearly present. Although this study illustrated limitations in discerning oxide thickness differences via depth profiling, statistically significant differences, when present, corresponded well with color/thickness correlations.

The thickness of the carbonaceous layers along the surface was not affected by the temperature of heat treatment. However, the CP surfaces had a thinner carbon layer, which reflects the higher γ_p values. Calcium, silicon, and sulfur thicknesses were minimal—these moieties were sputtered off within the first 2 sputtering cycles (about 3.4 Å). Unlike calcium and silicon, sulfur was present only on the Et surfaces; sulfur may have contributed to the lower surface energy values of Et specimens and may have contributed to the thickening of the surface oxide layer, broadening of the depth profile, or both.

Correlation coefficients, when significantly different from zero, were of similar magnitudes. Thus, only signs, ie, positive, negative, or no correlations, were examined, using CP only, Et only, and all specimens (Table 5). Although some significant correlations present in one of these groups were not

statistically significant with another, the signs were consistent when correlation coefficients were statistically significant for more than 1 group, eg, γ_p increased with oxide thickness for both CP-only and Et-only groups. Differences between the groups may be attributed to the difference in the number of specimens and the dependency of the correlation analysis on the range of the data examined (recall that the lowest of the γ_p values associated with the CP surface was higher than the largest value associated with the Et surfaces).

Although statistical correlation indicates association and not necessarily causation, the results suggest that polar forces at the specimen surface were dependent on the presence of the polar oxide present and any other polar moieties (such as adsorbed water) (see XPS section). Increased oxide thickness increased γ_p, but only to a point. Beyond a critical thickness, γ_p did not increase—γ_p values for 538CP and 427CP were similar. Polar forces are characteristic of moieties with fixed dipole moments and are inversely proportional to the fourth power of the distance—thus, polar forces act over a limited distance.[20,21] Hydrocarbons are ubiquitous; hence, despite the most stringent of cleaning procedures, carbonaceous layers are always present on surfaces, although the amount and composition of these layers are dependent on the specific cleaning protocols. Carbonaceous overlayers consisted predominantly of non-polar components (see XPS section below) that masked the polar forces from the underlying oxide layer. Non-polar (dispersive) forces tend to be more localized—they are inversely proportional to the seventh power of the distance from the source and are effective over a distance more limited than for polar forces.[20,21]

X-ray Photoelectron Spectroscopy

The survey and utility scans showed a comparable presence of titanium (19.8 ± 0.3%) and sodium (4.2 ± 1.0%) on all CP and Et surfaces. No temperature effects were seen on the relative percentages for any of the detected elements. Trace amounts of chlorine, nitrogen, calcium, phosphorus, and silicon were also observed. Differences in elements detected using Auger spectroscopy may be the result of different mean free paths of the respective characteristic electrons.[11]

The Et specimens showed a higher carbon and a lower oxygen content (Et: carbon = 25.4 ± 1.7%; oxygen = 51.0 ± 0.9%; CP: carbon = 19.0 ± 1.0%; oxygen = 54.4 ± 0.4%). This corroborates a previous study in which surfaces treated with ethanol were found to have a slightly, but statistically significantly, higher carbon content than untreated surfaces.[22] The amount of carbon in the samples from the current study was significantly lower than any of the surfaces examined previously, while the oxygen concentrations were significantly higher.[5] The titanium/oxygen ratios were > 2.0 for samples in this study and > 2.0 for samples in the previous study. This could have been caused by several factors, as follows: *(1)* the increased temperatures used in this study may have depleted the surface carbon layer; or *(2)* the thinner oxide layers in the previous study resulted in the spectra including a contribution from the underlying metallic titanium substrate, thereby increasing apparent titanium concentration and, as a consequence, decreased apparent oxygen content.

Because of the limited number of specimens, correlation coefficients determined using data from CP specimens only or Et specimens only were not significantly different from 0. When data from both groups were used, γ_p decreased with increasing surface concentration of carbon (ie, correlated negatively), as was the case with the combined Auger carbon depth profiles. The surface concentration of oxygen correlated positively with γ_t, ie, γ_t increased with increasing oxygen presence at the surface. This was consistent with Auger oxide thickness measurements, which correlated positively with γ_p and γ_t when only Et data were considered. Differences from Auger correlation analyses can be attributed to differences in sensitivity to specific elements, electron escape depths, possible sputtering artifacts, and characteristics used—that is, Auger correlations dealt with depth of elemental presence only and did not specifically consider concentration.

A sample high-resolution spectrum for the carbon 1s region is shown in Fig 3. Peak fitting showed 3 component peaks; there were no statistically significant differences in the corresponding peak positions between CP and Et surfaces (Table 6). The relative percentages of the peaks associated with the carbon subspecies were different for CP and Et surfaces. Peaks at ~289 eV and ~286 eV are associated with C=O (carbonyl) and C-O bonds, respectively. Peaks at ~285 eV are characteristic of aliphatic C-C, C-H bonds.[11,23] The amount of aliphatic C-C and C-H was the same for the Et and CP specimens. The CP specimens had a significantly greater amount of C-O species; this may be one reason for the higher γ_p values for the CP samples. Also, the shape of the ~286 eV peak for CP surfaces was broader, as determined by the FWHM parameter. Although a high FWHM can be indicative of lack of long-range order, the specific implication in this case is not clear.

The oxygen 1s envelope was fitted by 2 constitutive peaks; a representative plot is shown in Fig 4. All the samples had comparable sub-peak compositions: the 531.4 eV peak constituted 17 ± 1% and the 529.6

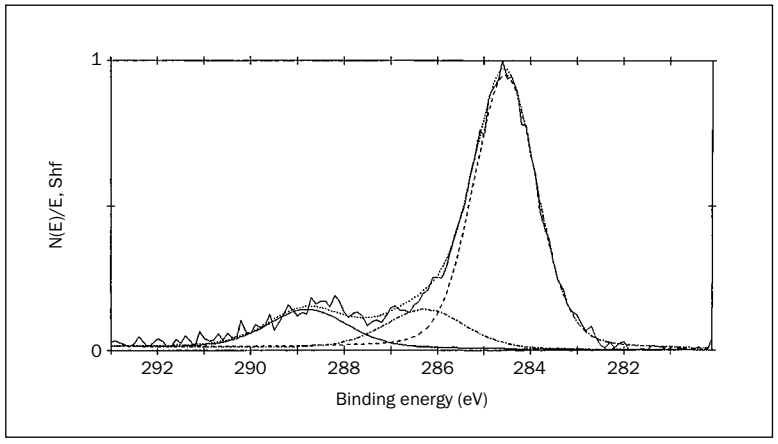

Fig 3 Deconvolution of XPS carbon envelope for 538CP specimens.

Table 6 Deconvoluted Carbon 1s Envelopes

		FWHM			FWHM			FWHM	
Specimen	**Peak I (eV)**	**eV**	**%**	**Peak II (eV)**	**eV**	**%**	**Peak III (eV)**	**eV**	**%**
CP	288.8 ± 0.2	2.0 ± 0.0	13 ± 1	286.3 ± 0.3	2.0 ± 0.0*	13 ± 1*	284.6 ± 0.0	1.6 ± 0.1	74 ± 0
Et	288.4 ± 0.1	2.3 ± 0.2	16 ± 2	286.3 ± 0.0	1.4 ± 0.0*	8 ± 1*	284.6 ± 0.0	1.6 ± 0.0	75 ± 1

*Significant difference between mean CP and mean Et.
FWHM = full-width half-maximum; CP = cleaned in phosphoric acid and passivated in nitric acid; Et = cleaned in ethanol.

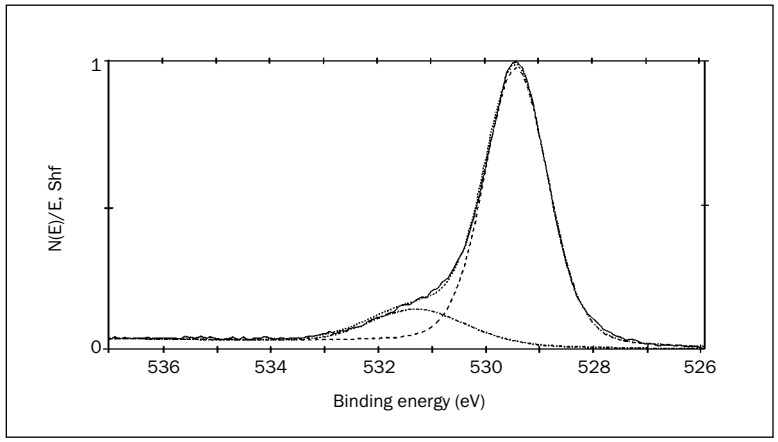

Fig 4 Deconvolution of XPS oxygen envelope of 538CP specimens.

eV made up 83 ± 1% of the oxygen envelope. The peak at the higher binding energy is characteristic of physisorbed water and the other of titanium dioxide.[24–29] There was no indication of peaks characteristic of chemisorbed OH peak at ~533 eV.[26] This was in contrast to specimens, examined in a previous study, that were not heat-treated or were heat-treated at a lower temperature than those studied in this investigation.[5] Desorption of undissociated chemisorbed water occurs at 380 K (107°C/225°F) and that of dissociated chemisorbed water occurs at 520 K (247°C/447°F), temperatures that were encountered in this study.[30] However, on cooling to room temperature, the environmental humidity may have resulted in readsorption of water. There are some concerns, however, that the ultra-high vacuum

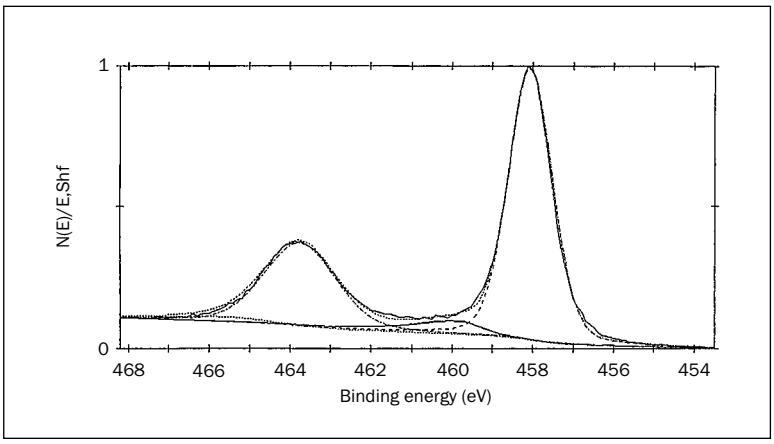

Fig 5 Deconvolution of XPS titanium doublet ($Ti2p_{3/2}$ and $Ti2p_{1/2}$) for 538CP specimens.

associated with XPS may rid the surface of physisorbed water. The oxygen peak at ~531.4 eV may also have been caused by carbonaceous material containing oxygen (C-OH and C=O)—corroborating the information from the high resolution carbon peaks or related to titanium sub-oxides.[11,25] All of the surfaces had similar oxide compositions.

High-resolution spectra of titanium peaks showed that the doublet peaks had a binding energy difference range of 5.7 to 5.9, further corroborating the presence of titanium dioxide (Fig 5).[31] There were no differences among the specimens. Also, peak fitting of the Ti $2p_{3/2}$ peak revealed only the peak at ~458.5 eV, which is characteristic of titanium oxide, unlike a previous study of CP specimens incubated at temperatures of 205°C or less, which detected the presence of Ti_2O_3 (~457 eV), and titanium metal (~454 eV).[32] This indicates that the oxide thicknesses of all the samples examined in this study were greater than the escape depth of photoelectrons from the underlying titanium substrate (and also from the intermediate Ti_2O_3 layer—see Raman spectroscopy section below).

Raman Spectroscopy

Raman scattering was observed for all of the surfaces heat-treated at 427°C and 538°C. Some of the specimens that were heat-treated at 316°C had broad peaks around 600, 840, and 914 cm^{-1}, as shown in Fig 6a. Absence of peaks at some sites suggested that surface oxide layer thickness was inadequate in certain areas for Raman signal detection. Raman spectroscopy examines a much greater depth than either XPS or AES, and the spectrum can be dominated by non-Raman signals from the metallic substrate.

The CP and Et surfaces heated to 427°C and 538°C were primarily rutile, with strong peaks at ~440 cm^{-1} and ~600 cm^{-1} and a smaller peak at ~840 cm^{-1} (Figs 6b and 6c).[33] Weaker peaks at ~250 cm^{-1} and ~330 cm^{-1} were attributed to Ti_2O_3; the literature cites values of ~254 to 271 cm^{-1} and ~332 to 347 cm^{-1} for these peaks.[34–37] These peaks do not indicate the presence of anatase because of the absence of characteristic Raman peaks at ~400 cm^{-1} and ~515 cm^{-1} for the 2 dominant anatase Raman peaks in the backscattering mode used in the current study.[38,39] Detector orientation was critical, as peaks at ~144 cm^{-1}, ~640 cm^{-1}, and 200 cm^{-1} are the dominant anatase peaks for perpendicular instrument detection geometries.[37–39] Peaks were not observed at these positions. Because XPS analysis is extremely surface-sensitive and did not detect any Ti_2O_3, the Ti_2O_3 detected with Raman spectroscopy was probably present below an outer titanium dioxide layer.

Titanium peroxide may have been present on all of the specimens, because all of the specimens showed a relatively prominent characteristic peak at ~914 cm^{-1}.[40] The supporting characteristic peak at 270 cm^{-1} may also have contributed to the ~250 cm^{-1} peak observed on all specimens. A peak at ~525 cm^{-1}, also characteristic of titanium peroxide, was observed with the CP specimens that were heat-treated for 30 minutes at 427°C. This peak was not observed on the other specimens because it may have overlapped with one of the rutile peaks (the one at ~600 cm^{-1}).

For specimens heat-treated at 427°C (800°F) and 538°C (1,000°F), the FWHM of the all peaks, except for at ~250 cm^{-1}, were less than 80 cm^{-1}.

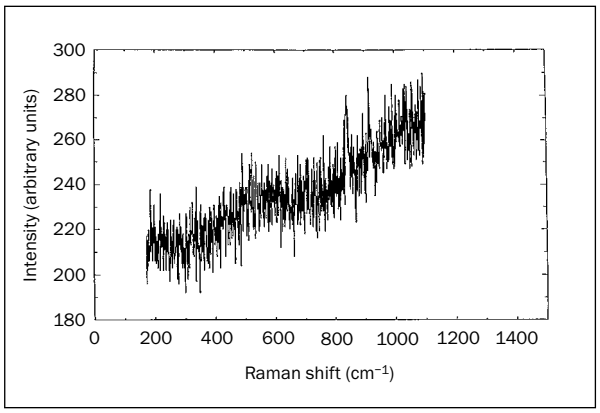

Fig 6a Representative Raman spectrum for surfaces heat-treated at 316°C.

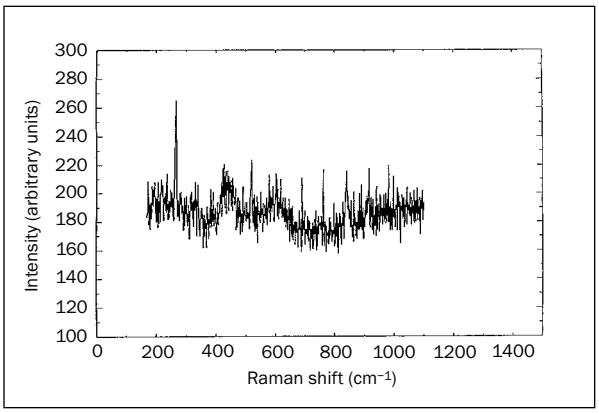

Fig 6b Representative Raman spectrum for surfaces heat-treated at 427°C.

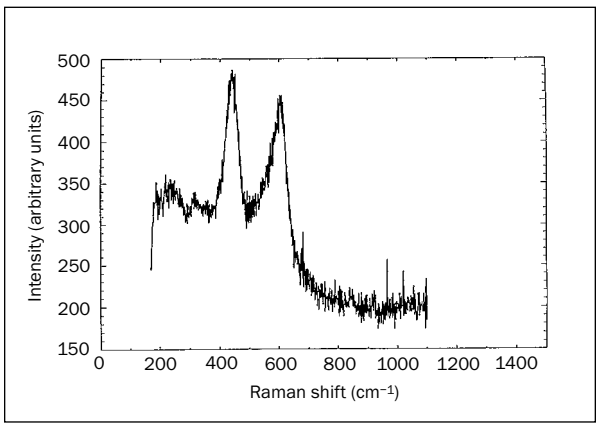

Fig 6c Representative Raman spectrum for surfaces heat-treated at 538°C.

This suggested that the titanium dioxide and Ti_2O_3 were both crystalline. Other investigators have ascribed absence of long-range order in titanium dioxide to FWHMs of ~180 cm^{-1} for the ~440 cm^{-1} peak and ~120 cm^{-1} for the ~600 cm^{-1} peak.[41] The width of the ~250 cm^{-1} peak could have been the result of an overlap of the rutile peak at ~240 cm^{-1} and the Ti_2O_3 or titanium peroxide peak at ~270 cm^{-1}.[33,40]

The characteristic peaks for rutile (~440 and ~600 cm^{-1}) were further examined for variations in specific peak positions. Analysis of variance, as well as correlation coefficients, showed that none of the variables (temperature or surface treatment) affected peak positions. Full-width half-maximums of the ~600 cm^{-1} peak, too, were not affected by these variables (65 ± 6 cm^{-1} at 427°C and 59 ± 6 cm^{-1} at 538°C). However, the FWHMs of the ~440 cm^{-1} peak, although not affected by surface treatment, decreased with increased heat-treatment temperature, from 68 ± 2 cm^{-1} at 427°C to 54 ± 2 cm^{-1} at 538°C. The FWHM is an indicator of grain size and structural defects; as calibration specific to the structural aspects of titanium oxides was not done, absolute grain sizes could not be determined. Heat treatment at 538°C would result in grains that were significantly larger than those resulting from heat treatment at 427°C.[41] Although increased temperatures resulted in higher surface energy, the concomitant increase in oxide crystallinity or oxide grain size may affect corrosion resistance.[19] Corrosion studies are currently underway to examine and optimize heat treatment protocols.

The results of this study indicate that there can be significant differences in surface energy based on the surface cleaning process—up to 10 dyn/cm—depending on whether a titanium surface was ethanol-cleaned or acid-cleaned and that these changes can be related to surface compositional changes. Clinicians sometimes resort to using ethanol as a quick sterilization process; this study shows that if so, significant implant surface changes may occur as a result. Previous studies have shown that in general for bone/dental implant success, higher surface energy surfaces are preferred.[42,43] For example, fibronectin reorganization and integrin binding of cells are associated with higher energy surfaces.[44] The specific in vivo outcomes for the processes examined in this investigation remain to be studied.

SUMMARY AND CONCLUSIONS

Implant-grade titanium specimens that were cleaned and passivated were rougher than the ethanol-cleaned surfaces. Analyses of solid surface tensions showed similar trends for polar and total solid surface tension values, which were significantly greater for the cleaned and passivated specimens; dispersive solid surface tension was not affected by the cleaning procdure or the temperature of heat treatment.

Spectroscopic analyses suggested that all of the surfaces had an outer oxide layer of TiO_2, an inner layer of Ti_2O_3, and possibly titanium peroxide. Variations of solid surface tension were related to differences in oxide thickness and crystallinity and in the area, thickness, and composition of carbonaceous presence within the surface zone. Although oxide thickness increased, as expected, with increasing heat treatment temperature, the cleaned and passivated samples had a thinner oxide and carbon depth measurement than the ethanol-cleaned specimens. The ethanol-cleaned specimens also had higher overall surface carbon concentrations. The carbonaceous layers on ethanol-cleaned specimens consisted of a chemical composition different from those on cleaned and passivated specimens. Thus, the various surface and heat treatments altered surface characteristics—surface compositions, surface roughness, and surface energies—and may have implications in clinical application. Studies are currently being conducted to further examine the effect of these differences on biologic interactions.

ACKNOWLEDGMENTS

This investigation was supported by NIDR Grant No. DE-08917. The AFM instrumentation was supported under Alabama EPSCOR Phase II. We thank Dr Edwin Bradley for his advice with the statistics; Mr Mark Koopman, Ms Cheri Moss, and Dr Robin Griffin for their help in the Auger laboratory; Dr Linda Lucas for the use of the Cahn dynamic contact angle analyzer; Mr Paul Lemons and Ms Krista Speer for their assistance with the logistics; and Dr John C. Gregory for his help.

REFERENCES

1. Albrektsson T, Jacobsson M. Bone-metal interface in osseointegration. J Prosthet Dent 1987;57:597–607.
2. Walivaara B, Aronsson B-O, Rodahl M, Lausmaa J, Tengvall P. Titanium with different oxides: *In vitro* studies of protein adsorption and contact activation. Biomaterials 1994;15(10): 827–834.
3. Den Braber ET, de Ruijter JE, Smits HTJ, Ginsel LA, von Recum AF, Jansen JA. Effect of parallel surface microgrooves and surface energy on cell growth. J Biomed Mater Res 1995;29:511–518.
4. ASTM. F86-91: Standard recommended practice for the preparation and marking of surgical implants. Volume 13, Section 13.01. Philadelphia: American Society for Testing and Biomaterials, 1995.
5. Kilpadi DV, Raikar GN, Liu J, Lemons JE, Vohra Y, Gregory JC. Effect of surface treatment on unalloyed titanium implants: Spectroscopic analyses. J Biomed Mater Res 1998; 40(4):646–659.
6. Kilpadi DV, Weimer JJ, Lemons JE. Effect of passivation and dry heat-sterilization surface energy and topography of unalloyed titanium implants. Colloids and Surfaces A: Physicochemical and Engineering Aspects 1998;135:89–101.
7. Ong JL, Lucas LC. Post-deposition heat treatments for ion beam sputter-deposited calcium phosphate coatings. Biomaterials 1994;15(5):337–341.
8. Kilpadi DV, Lemons JE. The effect of time on surface energy of unalloyed titanium implants. In: Proceedings of the Ninth Annual Alabama Materials Research Conference. Birmingham, AL: Alabama Materials Research Society, 1995.
9. Dalal EN. Calculation of solid surface tensions. Langmuir 1987;3:109–1015.
10. Wu S. Polymer Interface and Adhesion. New York: Marcel Dekker, 1982.
11. Lausmaa J, Kawemo B, Mattsson H. Surface spectrocopic characterization of titanium implant materials. Appl Surf Sci 1990;44:133–146.
12. Arnell RD, Davies PB, Halling J, Whomes TL, Tribology: Principles and Design Applications. London: MacMillan, 1991.
13. Black J. Biological Performance of Materials. Fundamentals of Biocompatibility, ed 2. New York: Marcel Dekker, 1992.
14. Wenzel RN. Resistance of solid surfaces to wetting by water. Ind Eng Chem 1936;28:988–994.
15. Kilpadi DV, Lemons JE. Surface energy characterization of unalloyed titanium implants. J Biomed Mater Res 1994;28: 1419–1425.
16. Fowkes FM. Determination of interfacial tensions, contact angles, and dispersion forces in surfaces by assuming additivity of intermolecular interactions in surface. J Phys Chem 1962;66:382.
17. Hofmann S. Depth profiling. In: Briggs D, Seah MP (eds). Practical Surface Analysis by Auger and X-ray Photoelectron Spectroscopy. New York: John Wiley & Sons Inc, 1983: 141–179.
18. Fukuzuka T, Shimogori K, Hiroshi S, Kamikubo F. On the beneficial effect of the titanium oxide film formed by thermal oxidation. In: Kimura H, Izumi O (eds). Titanium '80—Science and Technology Proceedings of the Fourth International Conference on Titanium. Warrendale, PA: Metallurgical Society of AIME, 1980:2783–2792.
19. Kilpadi DV, Lemons JE. The effect of surface and heat treatments on corrosion of unalloyed titanium implants. Proceedings of the 16th Southern Biomedical Engineering Conference. Biloxi, MS: 16th Southern Biomedical Engineering Conference, 1997.
20. Zisman WA. Relation of the equilibrium contact angle to liquid and solid constitution. In: Gould R (ed). Contact Angle, Wettability and Adhesion. Washington, DC: American Chemical Society, 1964:1–51.

21. Whitten KW, Gailey KD, Davis RE. General Chemistry with Qualitative Analysis. Philadelphia, PA: Saunders, 1988: 301–302.
22. Kilpadi DV. Surface Characterization of Unalloyed Titanium Implants [thesis]. Birmingham, AL: Univ of Alabama, 1996.
23. Ameen AP, Short RD, Johns R, Schwach G. The surface analysis of implant materials. 1. The surface composition of a titanium dental implant material. Clin Oral Implants Res 1993;4:144–150.
24. Ong JL, Lucas LC, Raikar GN, Connatser R, Gregory JC. Spectroscopic characterization of passivated titanium in a physiologic solution. J Mater Sci Mater Med 1995;6:113–119.
25. Kuznetsov MV, Zhuravlev JF, Zhilyaev VA, Gubanoz VA. XPS study of the nitrides, oxides, and oxynitrides of titania. J Electron Spectrosc Rel Phenomena 1992;58:1–9.
26. Healy KE, Ducheyne P. Oxidation kinetics of titanium thin films in model physiologic environments. J Colloid Interface Sci 1992;150(2):404–417.
27. Shirkhanzadeh M. XRD and XPS characterization of superplastic TiO_2 coatings prepared on Ti6A14V surgical alloy by an electrochemical method. J Mater Sci Mater 1995;6: 206–210.
28. Olejford I, Hansson S. Surface analysis of four dental implant systems. Int J Oral Maxillofac Implants 1993;8:32–40.
29. Sayer CN, Armstrong NR. X-ray photoelectron spectroscopy of TiO_2 and other titanate electrodes and various standard titanium oxide materials: Surface compositional changes of the TiO_2 electrode during photoelectrolysis. Surf Sci 1978;77:301–320.
30. Jobin M, Taborelli M, Emech R, Zenhausern F, Descouts P. Hydroxylation and crystallization of electropolished titanium surface. Ultramicroscopy 1992;42–44:637–643.
31. Hernández de Gatica NL, Jones GL, Gardella JA Jr. Surface characterization of titanium alloys sterilized for biomedical applications. Appl Surf Sci 1993;68:107–121.
32. Simon D, Devillers B, Bardeolle J. Study of the oxidation of titanium by microgravimetry and electron spectroscopy (ESCA) at elevated temperatures and low pressures. In: Kimura H, Izumi O (eds). Titanium '80—Science and Technology Proceedings of the Fourth International Conference on Titanium. Warrendale, PA: Metallurgical Society of AIME, 1980:2859–2866.
33. Pankuch M, Bell R, Melendres CA. Composition and structure of an anodic films on titanium in aqueous solutions. Electrochimica Acta 1993;38(18):2777–2779.
34. Mooradian A, Raccah PM. Raman study of the semiconductor-metal transition in Ti_2O_3. Phys Rev Bull 1971;3(12): 4253–4256.
35. Shin SH, Aggarwal RL, Lax B, Honig JM. Raman scattering in Ti_2O_3-V_2O_3 alloys. Phys Rev Bull 1974;9(2):583–590.
36. Fujii T, Sakata N, Takada J, Miura Y, Daitoh Y, Takano M. Characteristics of titanium oxide films deposited by an activated reactive evaporation technique method. J Mater Res 1994;9(6):1468–1473.
37. Franck M, Celis J-P, Roos JR. Microprobe Raman spectroscopy of TiN coatings oxidized by solar beam heat treatment. J Mater Res 1995;10(1):119–125.
38. Pawlewicz WT, Exarhos GJ, Conaway WE. Structural characterization of TiO_2 optical coatings by Raman spectroscopy. Appl Optics 1983;22(12):1837–1840.
39. Berger H. Tang H, Lévy F. Growth and Raman spectroscopic characterization of TiO_2 anatase single crystals. J Crystal Growth 1993;130:108–112.
40. Tengvall P, Vikinge TP, Lundström I, Liedburg B. FT-Raman spectroscopic studies of the degradation of titanium peroxy gels made from metallic titanium and hydrogen peroxide. J Colloid Interf Sci 1993;160:10–15.
41. Exarhos GJ. Molecular characterization of dielectric films by laser Raman spectroscopy. In: McGuire GE (ed). Characterization of Semiconductor Materials. Park Ridge, NJ: Noyes Publications, 1989:242–288.
42. Baier RE, Meyer AE, Natiella JR, Natiella RR, Carter JM. Surface properties determine bio-adhesive outcomes: Methods and results. J Biomed Mater Res 1984;18:337–355.
43. Uyen HM, van Dijk LJ, Busscher HJ. Adhesion of stainable, calcium-rich deposits on substrata with different surface-free energies. An in vivo study in beagle dogs. J Clin Periodontol 1989;16:393–397.
44. Altankov G, Grinnell F, Groth T. Studies on the biocompatibility of materials: Fibroblast reorganization of substratum-bound fibronectin on surfaces varying in wettability. J Biomed Mater Res 1996;30:385–391.